Table A. Summery of simulation results.

Compounds	V_m (cm^3/mol)	Std Error V_m (cm^3/mol)	V_{molec} (Å)	Std Error V_{molec} (Å)	MSA (Å)	Std Error MSA (Å)	Solvent-Solvent				$\lambda_{LJ}=0\rightarrow1$				$\lambda_C=0\rightarrow1$	
							E_{LJ}(inter) (kJ/mol)	Std Error E_{LJ}(inter)	E_C(inter) (kJ/mol)	Std Error E_C(inter)	$\Delta G^{\bullet}_{cav+insert}$ (kJ/mol)	Std Error $\Delta G^{\bullet}_{cav+insert}$ (kJ/mol)	E_{LJ}(inter) (kJ/mol)	E_{LJ}(inter) q=0 (kJ/mol)	Std Error E_{LJ}(inter) q=0	Std Error $\Delta G^{\bullet}_{charge}$ (kJ/mol)
acetaminophen	162.46	0.28	178.03	0.42	192.77	0.46	-90.70	0.21	-44.87	0.24	-4.41	2.09	-84.98	0.84	-22.59	0.51
acetylsalicylic acid	183.32	0.39	201.35	0.37	213.98	0.31	-103.68	0.27	-33.44	0.33	-13.58	1.23	-94.97	0.25	-16.54	0.24
atropine	345.35	1.20	352.57	0.61	351.50	0.61	-129.69	0.78	-12.48	0.33	-32.55	5.42	-115.29	8.05	-7.95	1.14
barbital	178.66	0.56	207.78	0.25	215.40	0.70	-123.57	0.33	-32.23	0.51	-17.83	4.24	-112.14	6.55	-12.31	0.79
benzocaine	201.70	1.31	201.07	0.04	217.37	0.60	-85.60	0.63	-23.58	0.17	-9.28	3.85	-80.69	1.12	-10.72	0.40
bifonazole	348.36	0.43	383.95	0.36	373.23	0.66	-165.37	0.20	-18.25	0.27	-20.64	1.26	-143.02	5.67	-10.25	0.77
caffeine	173.55	0.20	215.79	0.34	225.13	0.75	-154.18	0.30	-41.41	0.29	-20.19	4.56	-156.96	3.52	-21.21	1.85
chloramphenicol	278.25	1.00	308.55	0.26	321.44	0.67	-154.04	1.07	-57.60	0.52	-16.70	1.63	-131.07	6.10	-41.38	2.95
chlorpromazine	343.27	0.87	362.26	0.44	358.43	0.64	-152.09	0.70	-7.16	0.17	-42.31	1.84	-142.44	4.61	-5.04	0.95
cocaine	335.97	1.25	360.24	0.06	359.94	0.65	-151.28	0.74	-16.58	0.48	-20.49	2.91	-140.88	9.03	-8.92	0.82
codeine	310.55	1.18	339.81	0.54	323.63	0.66	-143.38	0.68	-12.45	0.23	-24.55	3.75	-132.01	4.10	-9.73	1.20
desipramine	328.97	0.67	342.51	0.19	338.09	0.63	-131.79	0.49	-7.22	0.09	-15.85	11.08	-117.97	4.09	-8.07	1.17
diazepam	277.48	1.35	316.59	0.11	310.77	0.69	-162.59	0.88	-17.17	0.28	-22.83	2.67	-145.62	1.47	-9.93	1.75
diethylstilbestrol	353.61	0.96	340.11	0.82	342.76	0.58	-107.06	0.38	-14.33	0.11	-10.91	3.85	-91.32	2.55	-7.73	0.26
estradiol	312.18	2.13	334.24	0.49	319.73	0.64	-131.47	1.16	-13.77	0.22	-24.57	0.45	-118.40	3.84	-7.18	1.17
ethyl-p-hydroxybenzoate	205.86	0.44	199.43	0.33	216.34	0.58	-82.36	0.27	-18.96	0.13	-13.84	0.81	-75.13	1.76	-9.04	0.45
fenbufen	275.62	1.32	303.62	0.59	307.98	0.66	-146.56	1.25	-24.28	0.25	-25.36	1.00	-139.50	3.78	-12.73	0.75
fenclofenac	288.27	0.29	298.24	0.29	304.49	0.62	-131.38	0.08	-15.97	0.04	-20.81	2.99	-120.45	2.07	-8.37	0.37
fluconazole	278.06	0.29	324.57	0.39	321.50	0.70	-166.52	0.42	-31.36	0.49	-21.07	8.12	-147.31	5.48	-17.21	0.52
flurbiprofen	276.78	1.34	282.45	0.02	285.71	0.61	-113.96	0.67	-15.89	0.12	-10.11	6.09	-106.48	1.07	-10.75	2.77
griseofulvin	349.56	1.08	371.61	0.24	373.06	0.64	-157.23	0.45	-20.35	0.56	-32.09	2.94	-144.50	1.47	-12.69	0.21
ibuprofen	300.36	2.05	270.80	0.29	283.07	0.54	-88.27	0.76	-9.80	0.12	-17.53	0.81	-78.46	1.97	-5.14	0.84
imipramine	358.14	2.54	366.56	0.43	362.14	0.62	-134.86	0.90	-5.02	0.17	-40.18	4.71	-117.52	6.84	-4.36	0.74
indomethacin	340.51	2.19	384.94	0.18	381.06	0.68	-191.16	1.80	-29.69	0.93	-22.28	4.53	-167.50	3.19	-17.34	1.41
indoprofen	274.19	0.26	324.32	0.20	321.92	0.71	-179.52	0.67	-41.17	0.37	-29.77	3.00	-170.03	2.27	-24.30	2.12
ketoprofen	276.26	0.72	302.64	0.43	305.45	0.66	-141.69	0.46	-25.00	0.42	-21.14	1.58	-129.51	1.68	-12.72	0.84
lidocaine	328.58	1.49	315.11	0.23	324.77	0.58	-103.53	0.44	-11.50	0.09	-13.84	7.03	-95.18	2.28	-5.06	2.53
lorazepam	274.85	1.30	317.06	0.20	311.07	0.69	-171.96	1.15	-29.52	0.56	-32.99	1.42	-163.16	4.29	-17.24	3.17
morphine	290.14	2.59	316.67	0.47	300.08	0.66	-137.30	1.48	-13.37	0.39	-31.95	8.19	-128.55	0.68	-6.24	1.86
naproxen	254.14	1.58	271.94	0.73	278.61	0.64	-122.35	0.88	-23.06	0.29	-19.64	1.15	-108.45	3.23	-12.96	0.35
nitrofurantoin	182.78	1.00	230.35	0.19	246.95	0.76	-182.19	0.90	-77.08	5.07	-8.24	4.04	-182.12	3.78	-37.34	1.15
oxazepam	261.60	1.78	301.94	0.33	297.10	0.70	-164.95	1.19	-29.36	0.10	-39.10	3.30	-148.90	6.76	-15.23	1.42
perphenazine	412.23	3.02	456.31	0.43	447.88	0.67	-207.82	2.60	-15.93	0.11	-38.28	9.88	-180.35	17.04	-11.69	1.75
phenacetin	221.58	0.71	223.60	0.41	240.81	0.61	-97.27	0.34	-28.14	0.28	-18.36	0.67	-89.27	1.82	-14.65	1.00
phenobarbital	216.58	1.56	257.18	0.13	254.75	0.72	-150.52	1.43	-35.47	1.99	-26.74	5.44	-142.54	6.54	-13.53	0.67
phenytoin	241.03	1.21	284.00	0.33	278.25	0.71	-154.79	0.88	-32.98	0.40	-20.09	2.52	-141.13	5.39	-16.01	0.93
procaine	298.27	1.04	301.07	0.52	315.27	0.61	-122.03	0.49	-18.81	0.15	-24.99	0.83	-111.88	4.80	-8.47	0.88
progesterone	365.05	1.14	399.44	1.27	374.39	0.66	-159.39	0.67	-11.01	0.14	-27.28	3.34	-148.48	3.99	-6.74	0.43
promazine	326.34	1.29	347.25	0.29	342.96	0.64	-141.88	0.76	-9.63	0.30	-41.51	1.42	-118.34	4.02	-6.13	1.21
prostaglandin E2	453.45	0.63	450.26	0.49	467.65	0.60	-157.87	0.46	-29.97	0.09	-19.67	3.65	-150.22	1.88	-16.30	1.27
salicylic acid	149.75	0.94	151.17	0.20	162.99	0.61	-71.74	0.51	-19.47	0.29	-11.90	1.01	-67.27	0.85	-10.39	3.78
sulindac	343.08	2.57	393.08	0.08	390.57	0.69	-184.19	2.07	-64.32	0.81	-14.20	7.07	-167.42	3.15	-33.96	3.51
testosterone	340.03	2.24	362.98	0.43	340.71	0.64	-137.57	1.26	-9.84	0.14	-25.85	1.81	-125.33	2.47	-4.75	0.59
trifluoperazine	419.22	2.27	446.00	0.37	438.39	0.64	-181.15	1.24	-8.54	0.38	-46.91	1.03	-154.81	5.95	-5.31	1.54
triflupromazine	377.91	0.77	381.73	0.41	378.93	0.61	-140.43	0.61	-8.29	0.28	-22.89	9.36	-127.82	4.15	-4.28	1.48
triclosan	279.61	1.72	268.32	0.34	276.79	0.58	-110.65	0.65	-4.87	0.18	-29.82	3.19	-101.74	3.01	-3.88	1.17

Note! The standard errors of the mean (Std error) are obtained from three independent simulations with different initial seed configuration.

To investigate the convergence in our obtained free energy results for pure melts we have divided the production sampling phase into two separate averages. These are then compared with each other as illustrated in Fig. A for the Coulomb decoupling step and in Fig. B for the Lennard-Jones decoupling step. In contrast to the data presented in Table A of the Supporting Information the changes of free energies in vacuum are not subtracted from the results presented in Fig. A and in Fig. B. The results presented in both these graphs confirm that the free energy changes have converged. For the Lennard-Jones decoupling step the uncertainties of calculated free energy changes are larger compared to the results from the Coulomb decoupling step. Still we cannot see any significant systematic deviation in the results shown in Fig. B. We have in a similar manner checked that the interaction energies have converged.

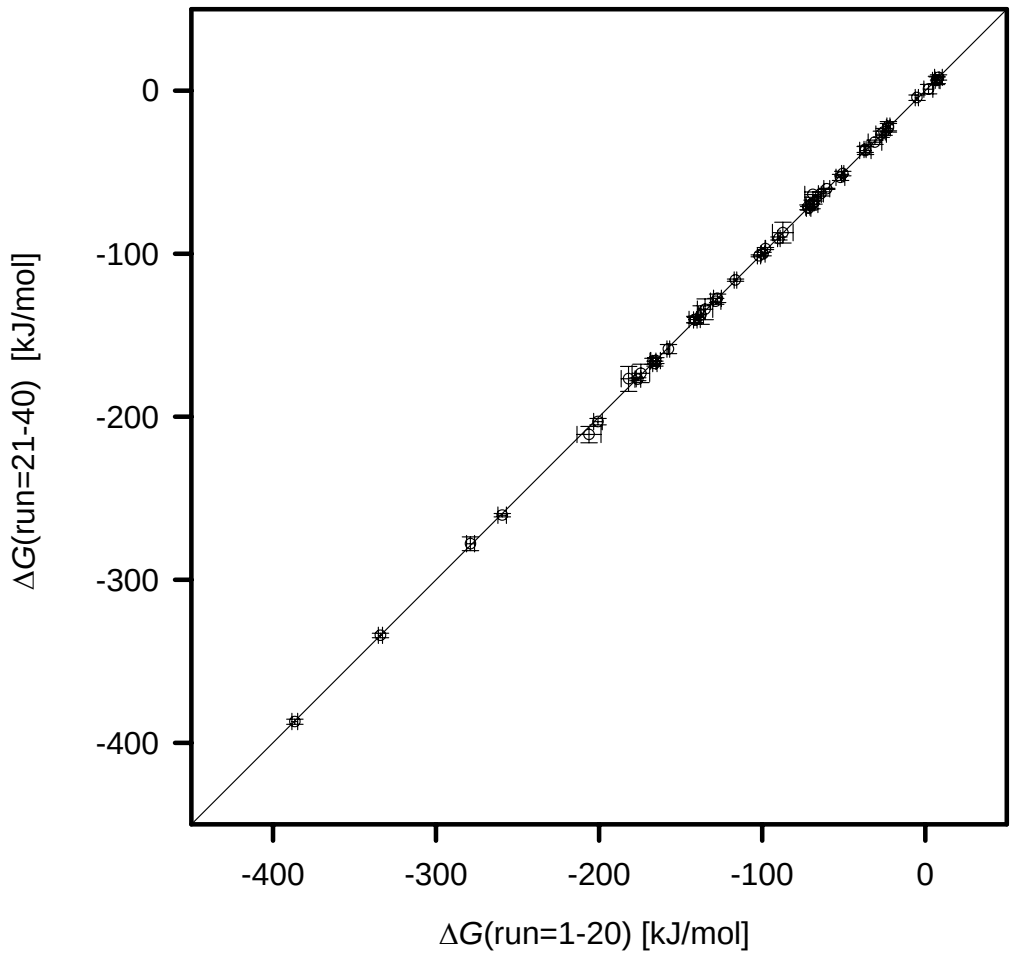

Figure A. The average results for the change in free energy of the partial charge decoupling step calculated from the final section of the production sampling is compared with corresponding results obtained from the first section. The symbols represent the averages and the error bars the standard deviations obtained from three independent simulations. Note that these results, in contrast to those in Table A, refers to data from which the corresponding free energy change in the vapor phase has not been subtracted.

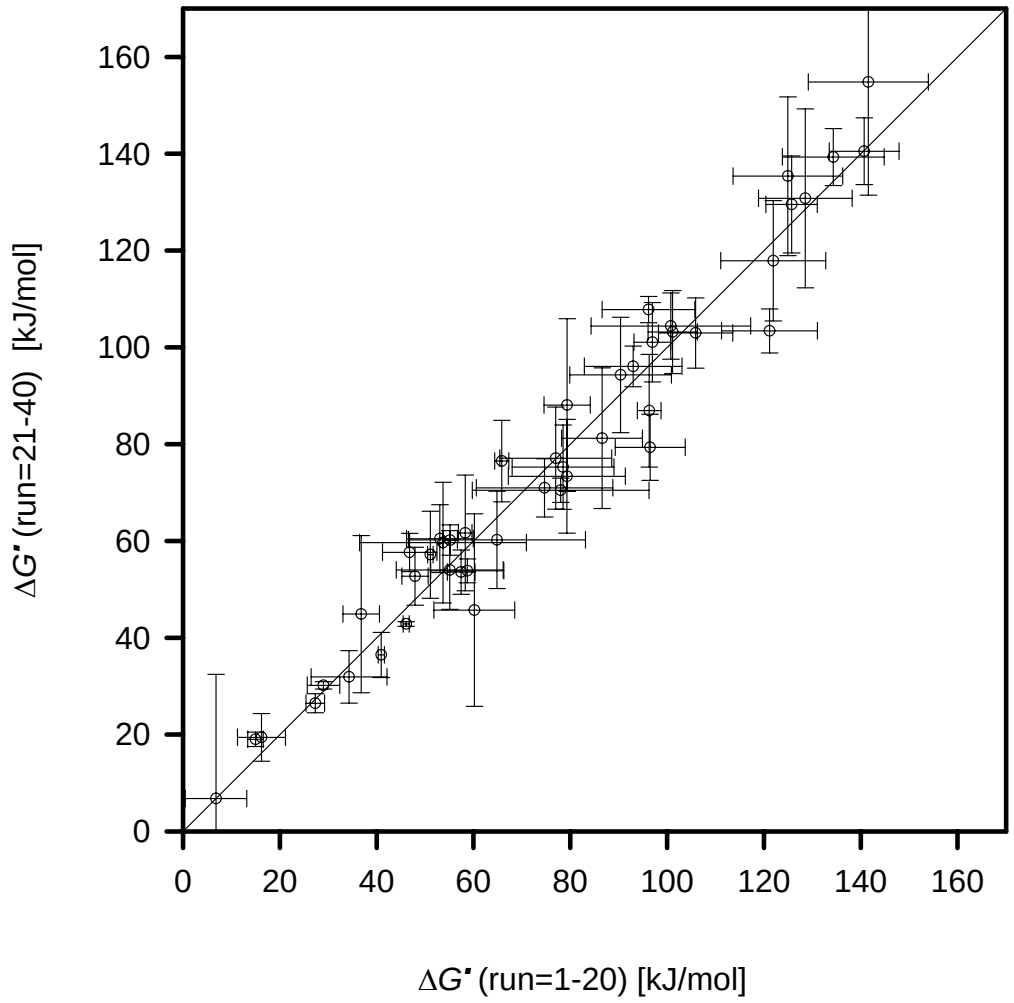

Figure B. The average results for the change in free energy of the Lennard-Jones decoupling step calculated from the final section of the production sampling is compared with corresponding results obtained from the first section. The symbols represent the averages and the error bars the standard deviations obtained from three independent simulations. Note that these results, in contrast to those in Table A, refers to data from which the corresponding free energy change in the vapor phase has not been subtracted.

In our performed free energy simulations we have used the so called double wide sampling procedure, which is considered an appropriate method to minimize hysteresis effects. Hysteresis effects in this respect means that there exists a memory impact when going from high λ (degree of coupling) on the simulations at lower λ. As such it would be ideal to run the simulations backwards and compare to the results. Since this would require a lot of work, we have instead performed simulations for three different molecules (atropine, desipramine and estradiol) where the equilibration time for each λ for the Lennard-Jones decoupling was increased up to ten-fold, to erase possible memory effects. From the results in figures C,D and E, it can be seen that there is no systematic trend in ΔG when the number of equilibration steps for each λ is increased tenfold.

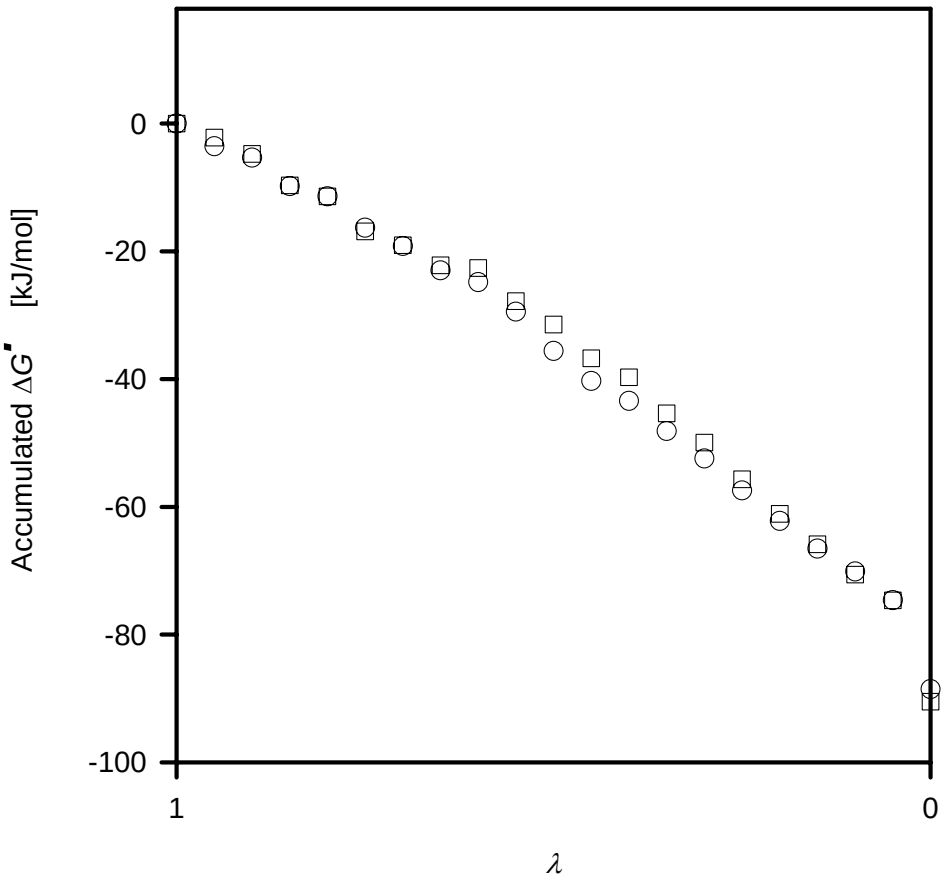

Figure C. The accumulated $\Delta G^{\bullet}$ results for an uncharged atropine molecule are shown when it is decoupled from the surrounding molecules by turning of the Lennard-Jones interaction. Note that the $\Delta G^{\bullet}$ changes due to the intramolecular decoupling are not subtracted here. At λ = 1, the alkane-like solute molecule interacts fully, via the Lennard-Jones interactions with the surrounding molecules and at λ = 0, the solute – solvent Lennard-Jones interactions are completely turned off and the molecule is shrunk to 10 % of its original size . The open circles represent results obtained from a standard performed simulation. To investigate the hysteresis effects of the Lennard-Jones decoupling results, the equilibration phase for each Lennard-

Jones decoupling window has been extended by factor of 10 in computation time and these results are presented by the open squares. Otherwise are the simulations performed identically.

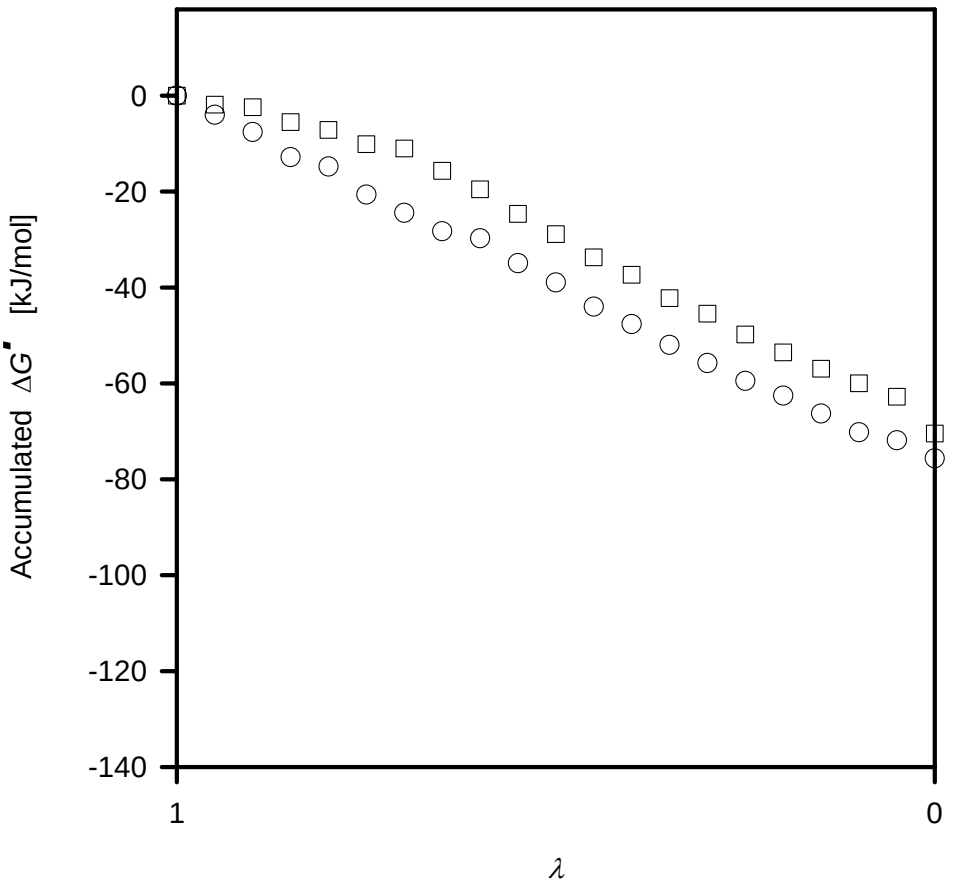

Figure D. The accumulated $\Delta G^{\bullet}$ results for an uncharged estradiol molecule are shown when it is decoupled from the surrounding molecules by turning of the Lennard-Jones interaction. Note that the $\Delta G^{\bullet}$ changes due to the intramolecular decoupling are not subtracted here. At λ = 1, the alkane-like solute molecule interacts fully via the Lennard-Jones interactions with the surrounding molecules and at λ = 0, the solute – solvent Lennard-Jones interactions are completely turned off and the molecule is shrunk to 10 % of its original size . The open circles represent results obtained from a standard simulation. To investigate the hysteresis effects of the Lennard-Jones decoupling results, the equilibration phase for each Lennard-Jones decoupling window has been extended by factor of 10 in computation time and these results are presented by the open squares. Otherwise are the simulations performed identically.

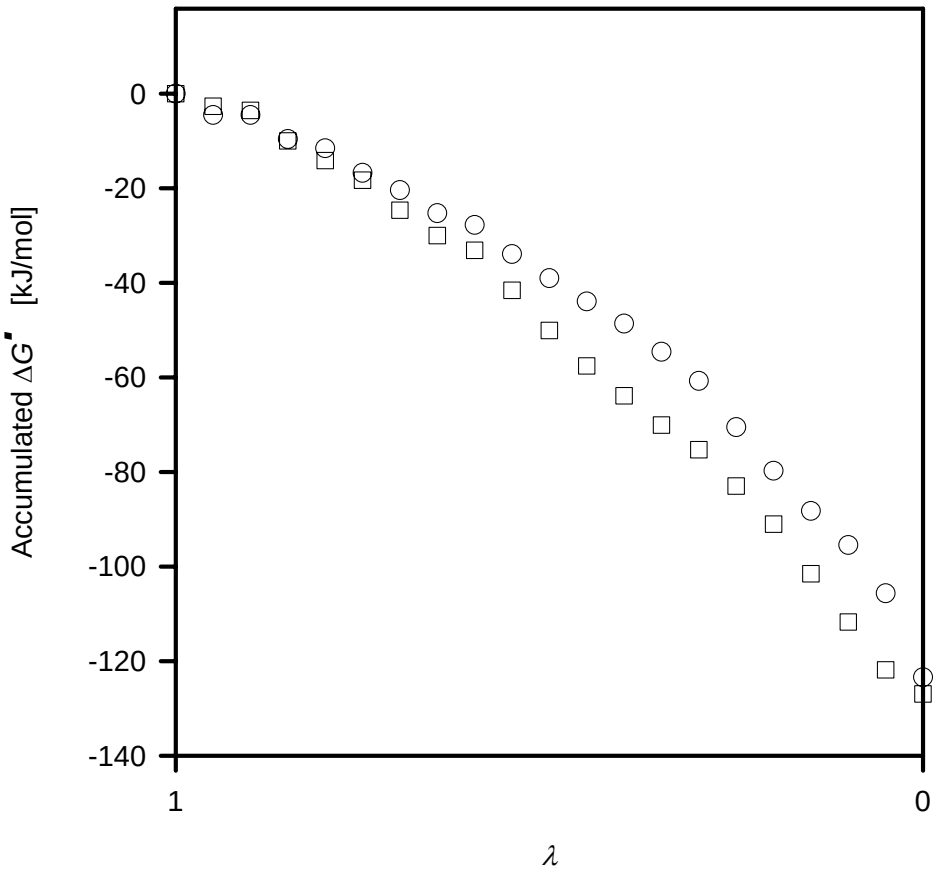

Figure E. The accumulated $\Delta G^{\bullet}$ results for an uncharged desiparmine molecule are shown when it is decoupled from the surrounding molecules by turning of the Lennard-Jones interaction. Note that the $\Delta G^{\bullet}$ changes due to the intramolecular decoupling are not subtracted here. At λ = 1, the alkane-like solute molecule interacts fully via the Lennard-Jones interactions with the surrounding molecules and at λ = 0, the solute – solvent Lennard-Jones interactions are completely turned off and the molecule is shrunk to 10 % of its original size . The open circles represent results obtained from a standard simulation. To investigate the hysteresis effects of the Lennard-Jones decoupling results, the equilibration phase for each Lennard-Jones decoupling window has been extended by factor of 10 in computation time and these results are presented by the open squares. Otherwise are the simulations performed identically.